Published in final edited form as:
*Prostaglandins Other Lipid Mediat*. 2014 October ; 0: 30–37. doi:10.1016/j.prostaglandins.2014.09.003.

# ROLE OF SOLUBLE EPOXIDE HYDROLASE IN AGE-RELATED VASCULAR COGNITIVE DECLINE

**Jonathan W. Nelson**[1,4], **Jennifer M. Young**[1], **Rohan Borkar**[1], **Randy L. Woltjer**[2], **Joseph F. Quinn**[3], **Lisa C. Silbert**[3], **Marjorie R. Grafe**[1,2], and **Nabil J. Alkayed**[1,3,4]

[1]Department of Anesthesiology & Perioperative Medicine, Oregon Health & Science University, Portland, OR 97239-3098, USA

[2]Department of Pathology, Oregon Health & Science University, Portland, OR 97239-3098, USA

[3]Layton Aging and Alzheimer's Disease Center, Department of Neurology, Oregon Health & Science University, Portland, OR 97239-3098, USA

[4]Knight Cardiovascular Institute, Oregon Health & Science University, Portland, OR 97239-3098, USA

## Abstract

P450 eicosanoids are important regulators of the cerebral microcirculation, but their role in cerebral small vessel disease is unclear. We tested the hypothesis that vascular cognitive impairment (VCI) is linked to reduced cerebral microvascular eicosanoid signaling. We analyzed human brain tissue from individuals formerly enrolled in the Oregon Brain Aging Study, who had a history of cognitive impairment histopathological evidence of microvascular disease. VCI subjects had significantly higher lesion burden both on premortem MRI and postmortem histopathology compared to age- and sex-matched controls. Mass spectrometry-based eicosanoid analysis revealed that 14,15-dihydroxyeicosatrienoic acid (DHET) was elevated in cortical brain tissue from VCI subjects. Immunoreactivity of soluble epoxide hydrolase (sEH), the enzyme responsible for 14,15-DHET formation, was localized to cerebral microvascular endothelium, and was enhanced in microvessels of affected tissue. Finally, we evaluated the genotype frequency of two functional single nucleotide polymorphisms of sEH gene EPHX2 in VCI and control groups. Our findings support a role for sEH and a potential benefit from sEH inhibitors in age-related VCI.

### Keywords

vascular cognitive impairment; soluble epoxide hydrolase; white matter hyperintensity; EPHX2; epoxyeicosatrienoic acids; EETs



To whom correspondence should be addressed: Nabil J. Alkayed, MD, PhD, Department of Anesthesiology & Perioperative Medicine, The Knight Cardiovascular Institute, Oregon Health & Science University, 3181 S.W. Sam Jackson Pk. Rd., UHN-2 Portland, Oregon 97239-3098, USA : Tel.: (503) 418-5502 ; Fax: (503) 494-3092; alkayedn@ohsu.edu.

## 1. Introduction

The World Health Organization estimates that 35.6 million people currently live with dementia, and that number is expected to double by 2030 and more than triple by 2050 [1]. Alzheimer's disease (AD) remains the most common cause of dementia, but the contribution of cerebrovascular pathology to AD and dementia in general is becoming more appreciated [2]. Indeed, recent autopsy studies have shown that nearly a third of individuals with dementia have co-morbid cerebrovascular pathologies [3,4]. Cerebrovascular pathology can be isolated or combined with AD pathology in the case of mixed-dementia. Recent efforts to create a set of criteria to delineate cognitive impairment, both mild and advanced dementia, which are attributable to cerebrovascular disease have led to the introduction of the term vascular cognitive impairment (VCI) [5],[6].

The most common type of VCI is that due to small vessel ischemic disease (also referred to as subcortical VCI ) [7]. Evidence of small vessel ischemic disease can be observed on T2-weighted magnetic resonance imaging (MRI) as hyperintensities primarily localized in white matter, both around the ventricles and as isolated foci. T2-white matter hyperintensity (WMH) is thought to reflect white matter lesions [8]. Consistent with a central role for small vessel disease in the development of dementia, a recent prospective study showed that acceleration in WMH volume changes was an early predictor of conversion to mild cognitive impairment [9].

Despite recent advances in characterizing VCI, mechanisms underlying the development of cerebral small vessel disease in VCI remain poorly understood. Arachidonic acid derivatives, collectively referred to as eicosanoids, play an important role in control of the cerebral microcirculation [10]. We, therefore, hypothesized that VCI is linked to impaired eicosanoid signaling. In particular, we were interested in the role of cytochrome P450-derived eicosanoids, since they have previously been linked to cerebrovascular function and disease [11]. For instance, elevated levels of 20-hydroxyeicosatetraenoic acid (20-HETE), a potent vasoconstrictor, have been linked to both ischemic and hemorrhagic strokes [12,13]. Conversely, elevated levels of 14,15-epoxyeicosatrienoic acids (14,15-EET), a vasodilator and neuroprotectant, have been shown to limit ischemic injury [14,15].

To test this hypothesis, we identified individuals with VCI and age- and sex-matched controls from the Oregon Brain Aging Study and quantified eicosanoid levels in cortical brain tissue biopsies using liquid chromatography-tandem mass spectroscopy (LC-MS/MS) [16]. We found higher levels of 14,15-dihydroxyeicosatrienoic acids (14,15-DHET), the inactive metabolic conversion product of 14,15-EET via the enzyme soluble epoxide hydrolase (sEH), in the VCI group. Consistent with a role in small vessel function and disease, sEH immunoreactivity was localized in cerebral microvascular endothelium, and was higher close to cerebrovascular lesions. Finally, we determined the frequency of functional single-polymorphisms polymorphisms (SNPs) in the sEH gene EPHX2 in both VCI and control subjects, which also correlated with WHM volume. While there have been some recent advances in our understanding of dementia, there are currently no effective treatments to limit or reverse the onset of dementia [17]. This work contributes to the

understanding of mechanisms underlying VCI and suggests a novel therapeutic strategy to treat VCI.

## 2. Materials and Methods

### 2.1 Ethics statement

The sources, collection, storage and distribution of information and biological specimens were in accordance with guidelines established by the Layton Center/ORCATECH Research Repository in compliance with Federal regulations and Oregon Health & Science University (OHSU) policies. For autopsy tissue, specific consent for research purposes was obtained from the next of kin as part of the consent for autopsy.

### 2.2 Study subjects

88 individuals were used for measurements of white matter hyperintensity (WMH) volume and for the genetic analysis were selected from the Oregon Brain Aging Study (OBAS) [16] based on the availability of DNA, T2-Weighted MRI measurements and neurocognitive assessment. All individuals in this study were Caucasian, except one, whose ethnicity is unknown. WMH volume measurements, mini mental state exams (MMSE), and clinical dementia ratings (CDR) were quantified as previously described [18].

Brains tissue used for immunohistochemistry and mass spectrometry-based analysis of eicosanoids was obtained from the Oregon Brain Bank and selected based on histopathological assessment performed by The Neuropathology Core of the Oregon Aging Alzheimer's Disease Center. VCI cases were selected based on previously described criteria of the Honolulu-Asia Aging Study [4], while controls were age-matched subjects that lacked microvascular ischemic injury as defined in that study. Specifically, VCI subjects were defined as those who had a high burden of microvascular lesions in either the neocortex or the basal ganglia and thalamus, or at both sites, while control subjects contained negligible microvascular lesions at both sites. Alzheimer's disease-related lesions (neuritic plaques and neurofibrillary tangles) were variable in subjects in both groups but were statistically matched. Cases containing Lewy bodies or other significant neurodegenerative disease-associated pathologies were excluded. Demographic data for individuals used for eicosanoid quantification are presented in Table 1. For one VCI individual, the post-mortem interval is unknown. Data for individuals used for immunohistochemistry are presented in Table 2.

### 2.3 LC-MS/MS analysis for eicosanoid metabolites

Post-mortem human brain samples were kept on dry ice until homogenization. Each sample was placed into 2.0 ml of PBS and then homogenized on ice using a polytron, at setting 2-3 for 20-30 seconds until homogenous. Samples were then diluted 1:1 with PBS. A 1 ml aliquot of the sample was mixed with 20 μl of an anti-oxidant mix consisting of 0.2mg/ml BHT, 2 mg/ml triphenyl phosphine, and 2 mg/ml indomethacin. Samples were then spiked with an internal standard mix consisting of 1 ng of each of the following, d8-15 HETE, d6-20 HETE, d8 14,15 EET, and d11-14,15 DHET. Samples were kept on dry ice prior to homogenization and wet ice at all times thereafter until hydrolysis. 1 ml of 15% KOH was added to each tube containing 1ml of the homogenized sample. The tube was briefly

vortexed, capped tightly, and then hydrolyzed at 40°C for 1 hour. Samples were cooled briefly (<=5 minutes) and then acidified with 200 µl of glacial acetic acid, and then pH checked using pH paper for a desired range of 3-4. Samples were extracted with 3 ml of ethyl acetate, followed by 3 ml of hexane:ethyl acetate 1:1, followed by 2 ml of hexane. The extracts were combined and dried under vacuum for 35 minutes at 35°C. 150 µl of 0.1N HCl was added to residue in each tube, followed by the addition of 1 ml of hexane. Samples were vortexed for 2× 20 sec, spun at 2000×g for 5 minutes and then hexane was transferred to a fresh tube. Samples were then dried under vacuum for approximately 7 minutes till dry and immediately brought up in 100 µl of start solvent which consisted of 45:55 (vol:vol) acetonitrile:water with 0.2 mg/ml TPP, 0.01% BHT and 0.01% formic acid and filtered through 0.22 micron placed in sample vials with inserts and analyzed immediately by LC-MS/MS. The injection volume was 20 µl. An un-extracted standard curve was used for these studies.

Levels of DHETs, HETEs and EETs were analyzed using a 5500 Q-TRAP hybrid/triple quadrupole linear ion trap mass spectrometer (Applied Biosystems) with electrospray ionization (ESI) in negative mode as described previously [19]. The mass spectrometer was interfaced to a Shimadzu (Columbia, MD) SIL-20AC XR auto-sampler followed by 2 LC-20AD XR LC pumps and analysis on an Applied Biosystems/SCIEX Q5500 instrument (Foster City, CA). The instrument was operated with the following settings: source voltage −4000 kV, GS1 40, GS2 40, CUR 35, TEM 450 and CAD gas HIGH. The scheduled MRM transitions monitored with a 1.5 minutes window are presented in Supplemental Table 1. Compounds were infused individually, and instrument parameters optimized for each multiple reaction monitoring transition. The gradient mobile phase was delivered at a flow rate of 0.5 ml per minute and consisted of two solvents, solution A, which consists of 0.05% acetic acid in water, and solution B, which consists of 0.05% acetic acid in acetonitrile. Initial concentration of solvent B was 45%, which was held for 0.1 minutes before it was increased to 60% over 5 minutes, then to 61.5% over 5 minutes, followed by an increase to 95% over 1.1 minutes. Solvent was then held at 95% for 2 minutes, decreased to 45% B over 0.4 minutes, then equilibrated for 5 minutes. The Betabasic-18 100 × 2, 3µm column was kept at 40 °C using a Shimadzu CTO-20AC column oven. Data was acquired and analyzed using Analyst 1.5.1 software. The standard curves covered a range from 0-1000 pg/sample and the limit of quantification was 10 pg per sample except for 19-HETE and 20-HETE, where the limit of quantification was 25 pg per sample and the relative standard deviation was less than 20%.

### 2.4 Assessment of vascular injury

Sections of frontal and temporal cortex with subcortical white matter, basal ganglia, and hippocampus were stained with hematoxylin and eosin (basal ganglia, hippocampus) or luxol fast blue/PAS (frontal, temporal). Sections were rated by a neuropathologist on the degree of arteriolosclerosis, perivascular hemosiderin leakage, perivascular space dilatation, and myelin loss according to previously published criteria [20]. We did not evaluate the degree of cortical amyloid angiopathy, as this is more commonly associated with AD changes rather than vascular dementia without AD, and could thus be a confounding factor in this study. Vascular injury was scored on these criteria as well as number of cortical

infarcts and neuron loss in the hippocampus on a scale of 0-3 as in Table 3. Each case was given a total score (sum of all scores for 4 brain regions) and a dichotomized score (score of 0 or 1 = 0 [normal or minimal pathology], score of 2 or 3 = 1 [significant pathology], such that the maximal possible total score was 48 and the maximal possible dichotomized score was 18, with higher scores indicating more severe vascular injury. While the sections were examined with coded numbers that did not identify the study group, this analysis cannot be considered completely “blinded,” as pathologic changes were evident in many sections.

### 2.5 Soluble epoxide hydrolase immunohistochemistry

Six micron thick sections of frontal cortex and subcortical white matter were stained using a rabbit polyclonal antibody to soluble epoxide hydrolase (anti-sEH, Sigma HPA023779). Sections were pretreated with citrate buffer, pH 6 in a steamer for 30 minutes to enhance antigenicity and with 3% hydrogen peroxide to reduce endogenous peroxidase activity. After reacting with biotinylated secondary antibody, the reaction was visualized using avidin-biotin-peroxidase complex (ABC kit, Vector) and diaminobenzidine. For negative controls the primary antibody was replaced by normal rabbit serum. To confirm endothelial localization of sEH, selected sections were stained using the fluorescent secondary antibody Cy3 and double labeled with either the endothelial marker CD31 (mouse anti-human CD31, Dako M0823) or the astrocytic marker GFAP (mouse anti-human GFAP Chemicon MAB360) with detection by a Cy5 conjugated secondary antibody. Fluorescent images were acquired on a Zeiss LSM 710 confocal microscope and images were adjusted for brightness and contrast using ImageJ.

### 2.6 Genotyping

DNA was extracted from patients as previously described [21]. The genotype of each subject for the K55R (rs41507953) and R287Q (rs751141) polymorphisms from the gene that encodes for sEH, EPHX2, was determined by allelic discrimination using TAQMAN technology (Invitrogen). After polymerase chain reaction, the fluorescent readings from the plate were detected on an ABI PRISM 700 according to the manufactures instructions (Applied Biosystems). Genotype was determined based on radial separation of population clusters on fluorescent intensity plots. Plasmids containing the human EPHX2 gene with either K55R or R287Q polymorphism were used as positive controls.

### 2.7 Statistics

Data are presented as the mean +/− SD or mean +/−SEM as indicated in figure legends. For WMH volume and unpaired Student’s t-test was used to compare groups. For MMSE, CDR and vascular score a Mann-Whitney non-parametric test was used to compare groups. Because eicosanoid concentrations do not follow a normal distribution, a Mann-Whitney non-parametric test was used to determine if differences between groups were statistically significant [13,22]. A Chi-squared test was used to evaluate differences in frequencies of polymorphisms between VCI and control groups. For comparisons of WMH volumes between EPHX2 genotypes, an unpaired Student’s t-test was used. Comparisons were considered significant if $p<0.05$.

# 3. Results

## 3.1 Vascular cognitive impairment cohort has increased white matter hyperintensity volume

We first set out to examine whether individuals from the Oregon Brain Aging Study (OBAS) identified to have VCI indeed carry an increased burden of white matter hyperintensity [16]. We first stratified individuals based on the presence or absence of vascular disease, as indicated by clinical notes, followed by additional stratification based on neurocognitive status (Fig. 1A). For individuals with vascular disease, we further selected individuals with at least mild cognitive impairment, as assessed by a mini mental state exam (MMSE) score of less than or equal to 27, a score previously shown to have the greatest sensitivity and specificity for detecting dementia in educated individuals [23]. These individuals were considered to have VCI. For individuals with no clinical evidence of vascular disease, we further selected individuals who were cognitively intact, based on a MMSE score greater than or equal to a score of 27. These individuals were considered as controls. Finally, VCI cases and controls subjects were age- and sex-matched based on demographic data collected at time of MRI (Fig. 1B).

Next we quantified the volume of WMH within each group (Fig. 1C). We found that the VCI group had significantly higher WMH volume than control group (Fig. 1D). This result is consistent with previously published reports showing an association between WMH volume and cognitive decline [24].

Additionally, we performed an extensive vascular assessment to determine the amount of cerebrovascular pathology within VCI brain compared to age-matched control brain based on previously published criteria summarized in Table 3 [20]. Our quantification included cerebrovascular pathology such as vascular thickening (Fig. 2A), dilation of perivascular space (Fig. 2B), and tissue rarefaction (Fig. 2C and 2D) which were combined into a comprehensive vascular score (see methods). As expected, we found that the amount of cerebrovascular pathology in the VCI brain is elevated compared to age-matched brains (Fig. 2E).

## 3.2 Elevated levels of dihydroxyeicosatrienoic acids in subjects with vascular cognitive impairment

Next we quantified eicosanoids from brain tissue of VCI and age-matched controls. We used a targeted lipidomic assay for oxidized fatty acids, which allows us to quantify metabolites listed in Supplemental Table 1, which are produced via the lipoxygenase (LOX) and P450 epoxygenase and hydrolase pathways. Of the panel of eicosanoids we quantified (Supplemental Table 2 and 3), the most striking difference between VCI and control brains was in the levels of dihydroxyeicosatrienoic acids (DHETs), which were significantly higher in VCI compared to control brains (Fig. 3A and D). Interestingly, we did not observe a difference in the levels of DHET precursor epoxyeicosatrienoic acids (EETs), which resulted in higher DHETs to EETs ratio in VCI compared to control brains (Fig. 2B and E). This ratio is often used as a surrogate marker for the activity of the enzyme soluble epoxide hydrolase (sEH), the main enzyme involved in the conversion of EETs to DHETs [25]. This

pattern was true for the sum of all EETs regioisomers (Fig. 3D, E, and F) as well as for individual regio-isomers 5,6-EET, 8,9-EET, 11,12-EET and 14,15-EET, the preferred substrate for sEH (Fig. 3A, B and C) [26,27].

Of the other metabolites that were quantified, we observed significant elevations in levels of LOX metabolites 5-HETE, 12-HETE, 18-HETE and P450 hydroxylase metabolite 20-HETE, but not 11-HETE or 15-HETE. Levels of 19-HETE were decreased, although the decrease was not statistically significant.

### 3.3 Soluble epoxide hydrolase expression in the aged human brain

To investigate the possibility that increased DHET levels in VCI brain were linked to increased expression of the enzyme sEH, we performed immunohistochemistry on brain tissue slices from VCI and age-matched control subjects. sEH immunoreactivity (sEH-IR) was localized in multiple cell types, most prominently, in microvessels, but also in astrocytes and neurons (Fig. 4A and C), consistent with previous reports [28]. Staining within blood vessels was consistent with endothelial localization and was stronger in small vs. large vessels (Fig. 4A and B). Contrary to previously published work, we did not detect sEH-IR in vascular smooth muscle (bracketed in Fig. 4B), but we did see it in peri-vascular adventitial cells (arrowheads in Fig. 4B). To confirm that microvascular sEH-IR was indeed endothelial and not from astrocyte end-feet, we performed double immunofluorescent labeling for sEH and the endothelial marker CD31 as well as the astrocyte marker GFAP. We found that sEH-IR co-localized with CD31 but not GFAP (Fig. 5A), which is consistent with previous published work showing sEH expression in endothelial cells isolated from mouse brain [29].

Next, we sought to determine if sEH vascular expression is higher in VCI than in control brains. We compared sEH-IR within each slice qualitatively, and observed that staining intensity was higher in microvessels near regions of microinfarction. The increase in sEH-IR was more pronounced in microvascular endothelium, and was not present in other cell types, such as neurons or astrocytes (Fig. 4D). Because of the localized nature of sEH-IR intensification near vascular lesions, measurements of overall staining intensity in sections diluted the localized differences between groups, resulting in no differences in overall intensities between the two groups, despite the fact that VCI brains have more lesions than control brains.

### 3.4 Association of functional sEH polymorphisms with VCI pathology

Finally, we examined whether polymorphisms in the gene that encodes for soluble epoxide hydrolase, EPHX2, is associated with VCI. We genotyped two single nucleotide polymorphisms (SNPs), which alter sEH protein sequence and affects its hydrolase enzymatic activity (Fig. 6A) [30]. Specifically we examined the K55R polymorphism (rs41507953), which has been shown to increase sEH activity, and the R287Q polymorphism (rs751141), which has been shown to decrease sEH activity [31]. In our study population, only one individual, in the control group, was a homozygous carrier for the R55 allele; all individuals were heterozygous Q287 carriers, with one individual in the control group being a compound heterozygote, carrying both a R55 and Q287 alleles.

In our sample size of 31 cases and 31 control subjects, we found no statistically significant differences in the genotype frequency of these polymorphisms between control and VCI groups, although the genotype frequency of R287Q polymorphism was more than 4 times higher in VCI vs. control groups (13% vs. 3%, p=0.12) (Fig. 6B).

We then evaluated the associations between these SNPs, WMH and VCI. We found that Q287 carriers, but not R55 carriers, have significantly higher WMH volume than do individuals who are WT at that locus (Fig. 6C and D). The association was true when combining control and VCI groups (N=62) as well as for all individuals in our OBAS cohort with DNA and MRI measurements (N=88, WT: 12.51 ± 1.72, Q287 carrier: 27.17 ± 11.02, p=.025). Because VCI status is associated with higher WMH (Fig. 1D), and VCI status exhibited a trend for association with Q287 carriers (Fig. 6B), it is possible that VCI status influenced the association between WMH volume and R287Q genotype. Therefore, to separate the effect of VCI, WMH volume in WT and Q287 carriers are presented separately for control and VCI groups in Supplemental Figure 1.

## 4. Discussion

In the United States, the cost of dementia has surpassed that of cancer and heart disease, increasing the urgency to understand the mechanisms underlying dementia to help identify new treatment strategies [32]. This study tested the hypothesis that VCI is linked to an imbalance in cerebral eicosanoid signaling. To our knowledge, this is the first study to quantify the levels of eicosanoid levels within aged human brain tissue, especially in aged human brain with dementia. This is also the first study to correlate sEH expression in human brain and its functional SNPs with VCI.

In quantifying eicosanoid levels, we found elevated levels of DHETs in the VCI compared to age-matched control brains. Interestingly, we did not observe a difference in the levels of EETs, suggesting that the elevation in DHETs levels was due to enhanced metabolism of EETs and not due to differences in their synthesis. Moreover, the DHETs / EETs ratio was found to be elevated in the VCI compared to age-matched control brains. The diol to epoxide ratio is a surrogate for sEH activity, with increases in the ratio indicative of higher sEH activity [33].

The finding that sEH activity is associated with VCI is consistent with previous work demonstrating that sEH activity plays a detrimental role in cerebrovascular diseases such as ischemic stroke [14,15]. Furthermore, studies have specifically linked sEH activity as being detrimental to cerebrovascular function [34]. Indeed, recent studies using a transgenic mouse have shown that overexpression of endothelial sEH is sufficient to cause vascular dysfunction [35]. This led us to investigate the expression of sEH within the VCI brain.

Our results of the expression pattern of sEH in the human brain were consistent with some but not all reports describing the cellular localization of sEH-IR [28]. Specifically, we found sEH-IR in vascular endothelium, neurons and astrocytes and adventitial cells, but did not find sEH in vascular smooth muscle. We made two interesting observations that are very relevant to VCI. First, that sEH-IR was more prominent in small vs. large vessel

endothelium, and second, that staining intensity was higher in microvessels adjacent to the microinfarction lesion characteristic of VCI than in distant normal microvessels. Whether the increase in sEH expression in microvascular endothelium contributes to or results from VCI needs to be determined in experimental studies.

Additionally, we found a significant association between R287Q SNP and the VCI linked pathology WMH. This was true for the 62 VCI cases and age-matched controls, and also when we expanded our study to examine all 88 individuals in which we had genotyping and WMH volume measurements. The significance of this association needs to be investigated in further studies, especially that studies have reported that this SNP has reduced catalytic active, and that it was protective against cardiovascular disease and stroke [11,31], both of which seem to contradict our finding of a positive association of R287Q with cerebrovascular white matter lesion and with sEH enzymatic activity. It should be pointed out that there have been conflicting reports as to whether or not this specific polymorphism is associated with increased or decreased risk of stroke in humans [36,37]. Furthermore, the effect of this polymorphism on sEH function is complex. It has been shown to decrease both hydrolase and phosphatase catalytic activities, disrupt protein homodimerization, as well as enhance peroxisome translocation [30,38-40].

In our limited sample size of 62, we did not observe a statistically significant difference in the frequency of K55R or R287Q polymorphisms between VCI and control groups. This would suggest that the elevated DHETs levels in the VCI brain cannot be attributed to functional polymorphisms in the sEH gene. However, consistent with its association with WMH, the frequency of R287Q polymorphism was more than 4 times higher in VCI vs. the control group.

The study has a number of limitations. First, it is a retrospective study that relied on the availability of previously archived samples from tissue repositories. Future studies will be made stronger by prospectively following the progression of WMH volume changes in individuals with predefined EPHX2 genotypes. The second limitation is the limited sample size of this study. As larger cohorts become available, we will continue to study the genetic association between sEH SNPs and VCI. Finally, this study used post-mortem brain tissue to examine eicosanoid levels and sEH expression patterns, which is an unavoidable limitation when studying human brain tissue.

In conclusion, we made the following novel observations: 1) DHET levels are elevated in brain tissue from individuals with VCI, 2) immunoreactivity for sEH was localized to cerebral microvascular endothelium, and was higher in microvessels adjacent to lesions characteristic of VCI, 3) the R287Q polymorphism of sEH was associated with increased WMH volume. These findings suggest that sEH is involved in VCI pathology. Future mechanistic studies in animal models of VCI are needed to determine a causative role for sEH in the development and progression of VCI. Nevertheless, the finding that the VCI brain is associated with increased sEH activity suggests that sEH inhibitors may be beneficial for the prevention and treatment of VCI [41].

## Supplementary Material

Refer to Web version on PubMed Central for supplementary material.

## Acknowledgments

This work was supported by funds from the NIH grant R21 AG043857 (NJA) and P30 AG008017. We would also like to thank the Oregon Brain Aging Study (OBAS; PI: Kaye; supported by Department of Veterans Affairs, P30 AG008017, UL1 RR024140) and the Oregon Alzheimer Disease Center (Director: Kaye; P30 AG008017) for providing access to control and VCI samples and data. Additionally, we would like to acknowledge the University Shared Resource Program and the BSR/PKCore for the assistance with the eicosanoid quantification. We also wish to acknowledge Stefanie Kaech-Petrie and the Advanced Light Microscopy Core at The Jungers Center for technical assistance with fluorescence image acquisition. Finally, we would like to thank all of the research participates who made this study possible.

## Abbreviations

| | |
|---|---|
| **OBAS** | Oregon Brain Aging Study |
| **WMH** | T2 White Matter Hyperintensity |
| **MRI** | Magnetic Resonance Imaging |
| **MMSE** | Mini-Mental State Exam |
| **CDR** | Clinical Dementia Rating |
| **VCI** | Vascular Cognitive Impairment |
| **EETs** | Epoxyeicosatrienoic Acids |
| **DHETs** | Dihydroxyeicosatrienoic Acids |
| **HETEs** | hydroxyeicosatetraenoic acids |
| **AD** | Alzheimer’s Disease |
| **SNP** | Single Nucleotide Polymorphism |

## References

[1]. World Health Organization. Dementia: a public health priority. WHO; 2012.

[2]. Thies W, Bleiler L. 2013 Alzheimer’s disease facts and figures. Alzheimers Dement. 2013; 9:208–45. [PubMed: 23507120]

[3]. Knopman DS, Parisi JE, Boeve BF, Cha RH, Apaydin H, Salviati A, et al. Vascular dementia in a population-based autopsy study. Arch Neurol. 2003; 60:569–75. [PubMed: 12707071]

[4]. White L, Petrovitch H, Hardman J, Nelson J, Davis DG, Ross GW, et al. Cerebrovascular pathology and dementia in autopsied Honolulu-Asia Aging Study participants. Ann N Y Acad Sci. 2002; 977:9–23. [PubMed: 12480729]

[5]. Iadecola C. The pathobiology of vascular dementia. Neuron. 2013; 80:844–66. [PubMed: 24267647]

[6]. Gorelick PB, Scuteri A, Black SE, DeCarli C, Greenberg SM, Iadecola C, et al. Vascular Contributions to Cognitive Impairment and Dementia: A Statement for Healthcare Professionals From the American Heart Association/American Stroke Association. Stroke. 2011; 42:2672–713. [PubMed: 21778438]

[7]. Bowler JV. Modern concept of vascular cognitive impairment. Br Med Bull. 2007; 83:291–305. [PubMed: 17675645]

[8]. Kanekar S, Poot JD. Neuroimaging of vascular dementia. Radiol Clin North Am. 2014; 52:383–401. [PubMed: 24582345]

[9]. Silbert LC, Dodge HH, Perkins LG, Sherbakov L, Lahna D, Erten-Lyons D, et al. Trajectory of white matter hyperintensity burden preceding mild cognitive impairment. Neurology. 2012; 79:741–7. [PubMed: 22843262]

[10]. Imig JD, Simpkins AN, Renic M, Harder DR. Cytochrome P450 eicosanoids and cerebral vascular function. Expert Rev Mol Med. 2011; 13:e7. [PubMed: 21356152]

[11]. Iliff JJ, Jia J, Nelson J, Goyagi T, Klaus J, Alkayed NJ. Epoxyeicosanoid signaling in CNS function and disease. Prostaglandins Other Lipid Mediat. 2010; 91:68–84. [PubMed: 19545642]

[12]. Dunn KM, Renic M, Flasch AK, Harder DR, Falck J, Roman RJ. Elevated production of 20-HETE in the cerebral vasculature contributes to severity of ischemic stroke and oxidative stress in spontaneously hypertensive rats. Am J Physiol Heart Circ Physiol. 2008; 295:H2455–65. [PubMed: 18952718]

[13]. Crago EA, Thampatty BP, Sherwood PR, Kuo C-WJ, Bender C, Balzer J, et al. Cerebrospinal fluid 20-HETE is associated with delayed cerebral ischemia and poor outcomes after aneurysmal subarachnoid hemorrhage. Stroke. 2011; 42:1872–7. [PubMed: 21617146]

[14]. Zhang W, Otsuka T, Sugo N, Ardeshiri A, Alhadid YK, Iliff JJ, et al. Soluble epoxide hydrolase gene deletion is protective against experimental cerebral ischemia. Stroke. 2008; 39:2073–8. [PubMed: 18369166]

[15]. Zhang W, Koerner IP, Noppens R, Grafe M, Tsai H-J, Morisseau C, et al. Soluble epoxide hydrolase: a novel therapeutic target in stroke. J Cereb Blood Flow Metab. 2007; 27:1931–40. [PubMed: 17440491]

[16]. Green MS, Kaye JA, Ball MJ. The Oregon brain aging study: neuropathology accompanying healthy aging in the oldest old. Neurology. 2000; 54:105–13. [PubMed: 10636134]

[17]. Reiman EM. Alzheimer's disease and other dementias: advances in 2013. Lancet Neurol. 2014; 13:3–5. [PubMed: 24331781]

[18]. Silbert LC, Nelson C, Howieson DB, Moore MM, Kaye JA. Impact of white matter hyperintensity volume progression on rate of cognitive and motor decline. Neurology. 2008; 71:108–13. [PubMed: 18606964]

[19]. Iliff JJ, Fairbanks SL, Balkowiec A, Alkayed NJ. Epoxyeicosatrienoic acids are endogenous regulators of vasoactive neuropeptide release from trigeminal ganglion neurons. J Neurochem. 2010; 115:1530–42. [PubMed: 20950340]

[20]. Deramecourt V, Slade JY, Oakley AE, Perry RH, Ince PG, Maurage CA, et al. Staging and natural history of cerebrovascular pathology in dementia. Neurology. 2012; 78:1043–50. [PubMed: 22377814]

[21]. Kramer PL, Xu H, Woltjer RL, Westaway SK, Clark D, Erten-Lyons D, et al. Alzheimer disease pathology in cognitively healthy elderly: a genome-wide study. Neurobiol Aging. 2011; 32:2113–22. [PubMed: 20452100]

[22]. Siler DA, Martini M, Ward J, Nelson J, Borkar R, Zuioaga K, et al. Protective Role of P450 Epoxyeicosanoids in Subarachnoid Hemorrhage. Neurocrit Care. In press.

[23]. O'Bryant SE, Humphreys JD, Smith GE, Ivnik RJ, Graff-Radford NR, Petersen RC, et al. Detecting dementia with the mini-mental state examination in highly educated individuals. Arch Neurol. 2008; 65:963–7. [PubMed: 18625866]

[24]. Dufouil C, Godin O, Chalmers J, Coskun O, MacMahon S, Tzourio-Mazoyer N, et al. Severe cerebral white matter hyperintensities predict severe cognitive decline in patients with cerebrovascular disease history. Stroke. 2009; 40:2219–21. [PubMed: 19390070]

[25]. Zhao X, Yamamoto T, Newman JW, Kim I-H, Watanabe T, Hammock BD, et al. Soluble epoxide hydrolase inhibition protects the kidney from hypertension-induced damage. J Am Soc Nephrol. 2004; 15:1244–53. [PubMed: 15100364]

[26]. Yu Z, Xu F, Huse LM, Morisseau C, Draper AJ, Newman JW, et al. Soluble epoxide hydrolase regulates hydrolysis of vasoactive epoxyeicosatrienoic acids. Circ Res. 2000; 87:992–8. [PubMed: 11090543]

[27]. Jiang H, Zhu AG, Mamczur M, Morisseau C, Hammock BD, Falck JR, et al. Hydrolysis of cis- and trans-epoxyeicosatrienoic acids by rat red blood cells. J Pharmacol Exp Ther. 2008; 326:330–7. [PubMed: 18445784]

[28]. Sura P, Sura R, Enayetallah AE, Grant DF. Distribution and expression of soluble epoxide hydrolase in human brain. J Histochem Cytochem. 2008; 56:551–9. [PubMed: 18319271]

[29]. Gupta NC, Davis CM, Nelson JW, Young JM, Alkayed NJ. Soluble epoxide hydrolase: sex differences and role in endothelial cell survival. Arterioscler Thromb Vasc Biol. 2012; 32:1936–42. [PubMed: 22723436]

[30]. Przybyla-Zawislak BD, Srivastava PK, Vazquez-Matias J, Mohrenweiser HW, Maxwell JE, Hammock BD, et al. Polymorphisms in human soluble epoxide hydrolase. Mol Pharmacol. 2003; 64:482–90. [PubMed: 12869654]

[31]. Koerner IP, Jacks R, DeBarber AE, Koop D, Mao P, Grant DF, et al. Polymorphisms in the human soluble epoxide hydrolase gene EPHX2 linked to neuronal survival after ischemic injury. J Neurosci. 2007; 27:4642–9. [PubMed: 17460077]

[32]. Hurd MD, Martorell P, Delavande A, Mullen KJ, Langa KM. Monetary costs of dementia in the United States. N Engl J Med. 2013; 368:1326–34. [PubMed: 23550670]

[33]. Shao Z, Fu Z, Stahl A, Joyal J-S, Hatton C, Juan A, et al. Cytochrome P450 2C8 ω3-long-chain polyunsaturated fatty acid metabolites increase mouse retinal pathologic neovascularization--brief report. Arterioscler Thromb Vasc Biol. 2014; 34:581–6. [PubMed: 24458713]

[34]. Simpkins AN, Rudic RD, Schreihofer D, Roy S, Manhiani M, Tsai H-J, et al. Soluble epoxide inhibition is protective against cerebral ischemia via vascular and neural protection. Am J Pathol. 2009; 174:2086–95. [PubMed: 19435785]

[35]. Zhang W, Davis CM, Edin ML, Lee CR, Zeldin DC, Alkayed NJ. Role of endothelial soluble epoxide hydrolase in cerebrovascular function and ischemic injury. PLoS One. 2013; 8:e61244. [PubMed: 23585883]

[36]. Gschwendtner A, Ripke S, Freilinger T, Lichtner P, Müller-Myhsok B, Wichmann H-E, et al. Genetic variation in soluble epoxide hydrolase (EPHX2) is associated with an increased risk of ischemic stroke in white Europeans. Stroke. 2008; 39:1593–6. [PubMed: 18323494]

[37]. Zhang L, Ding H, Yan J, Hui R, Wang W, Kissling GE, et al. Genetic variation in cytochrome P450 2J2 and soluble epoxide hydrolase and risk of ischemic stroke in a Chinese population. Pharmacogenet Genomics. 2008; 18:45–51. [PubMed: 18216721]

[38]. Luo B, Norris C, Bolstad ESD, Knecht DA, Grant DF. Protein quaternary structure and expression levels contribute to peroxisomal-targeting-sequence-1-mediated peroxisomal import of human soluble epoxide hydrolase. J Mol Biol. 2008; 380:31–41. [PubMed: 18513744]

[39]. Srivastava PK, Sharma VK, Kalonia DS, Grant DF. Polymorphisms in human soluble epoxide hydrolase: effects on enzyme activity, enzyme stability, and quaternary structure. Arch Biochem Biophys. 2004; 427:164–9. [PubMed: 15196990]

[40]. Nelson JW, Subrahmanyan RM, Summers S a, Xiao X, Alkayed NJ. Soluble Epoxide Hydrolase Dimerization is Required For Hydrolase Activity. J Biol Chem. 2013; 288:7697–703. [PubMed: 23362272]

[41]. Shen HC. Soluble epoxide hydrolase inhibitors: a patent review. Expert Opin Ther Pat. 2010; 20:941–56. [PubMed: 20429668]

[42]. Gomez GA, Morisseau C, Hammock BD, Christianson DW. Structure of human epoxide hydrolase reveals mechanistic inferences on bifunctional catalysis in epoxide and phosphate ester hydrolysis. Biochemistry. 2004; 43:4716–23. [PubMed: 15096040]

## Highlights

- Vascular cognitive impairment (VCI) is associated with higher cerebrovascular lesion burden both on premortem MRI and postmortem histopathology.
- Levels of 14,15-dihydroxyeicosatrienoic acid (14,15-DHET) are elevated in human VCI brain tissue.
- Soluble epoxide hydrolase immunoreactivity is localized in microvascular endothelium in human brain and is higher in microvessels adjacent to lesions.
- EPHX2 polymorphism R287Q is associated with higher volume of $T_2$-weighted white mater hyperintensity.

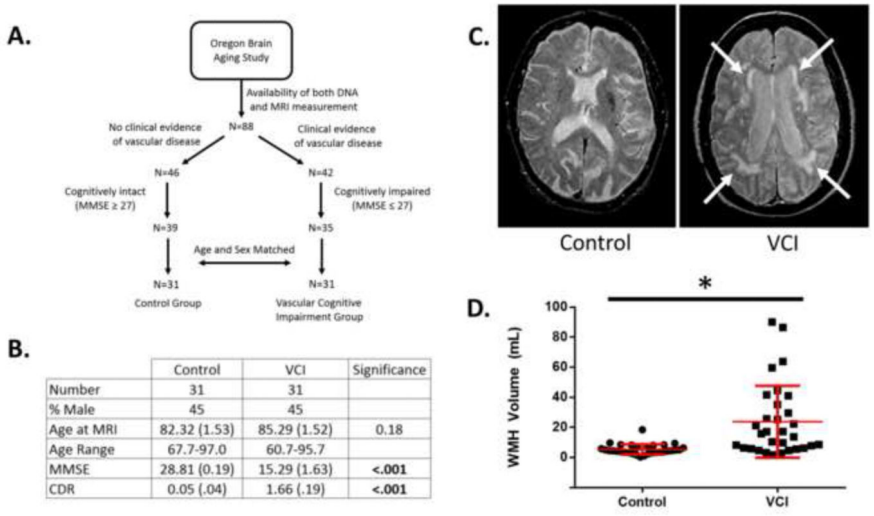


B.

| | Control | VCI | Significance |
|---|---|---|---|
| Number | 31 | 31 | |
| % Male | 45 | 45 | |
| Age at MRI | 82.32 (1.53) | 85.29 (1.52) | 0.18 |
| Age Range | 67.7-97.0 | 60.7-95.7 | |
| MMSE | 28.81 (0.19) | 15.29 (1.63) | **<.001** |
| CDR | 0.05 (.04) | 1.66 (.19) | **<.001** |

**Figure 1. Phenotypic characterization of vascular cognitive impairment (VCI)**

A. Selection criteria for subjects in the control and VCI groups. B. Demographic and neurocognitive characteristics of VCI and control groups. C. Representative T2-weighted MRI scans of a control and VCI subjects. White arrows indicate areas of WMH. D. Quantification of WMH volume in control and VCI groups. WMH Graph is a dot plot of each subject with mean +/− SD in red, whereas values in the table are mean +/− SEM. Differences in age and WMH were evaluated by unpaired Student's t-test, and differences in MMSE and CDR were evaluated by a non-parametric Mann-Whitney test. * signifies $p<.05$.

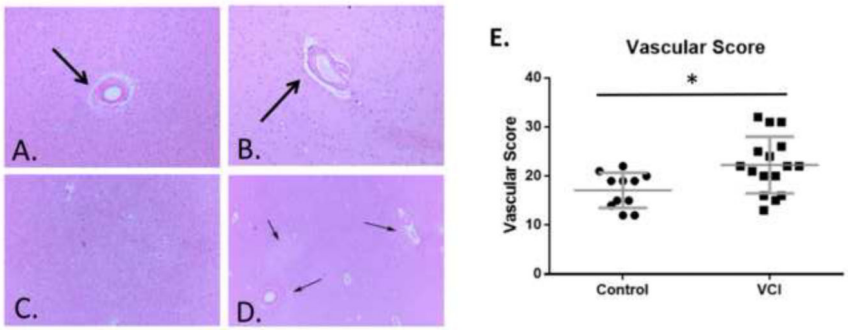


**Figure 2. Histopathological characterization of control and VCI brain tissue**

Examples of vascular thickening (arrow, A.), dilated perivascular space (arrow B.), diffuse white matter rarefaction (C.), and multifocal rarefaction (arrows, D.) in aged human brain tissue. E. Comprehensive histopathological score of cerebrovascular pathology in control and VCI brain. n = 11 for control and n=16 separate brains for VCI group. Significance was determined by a Mann-Whitney non-parametric test. * indicates $p<.05$.

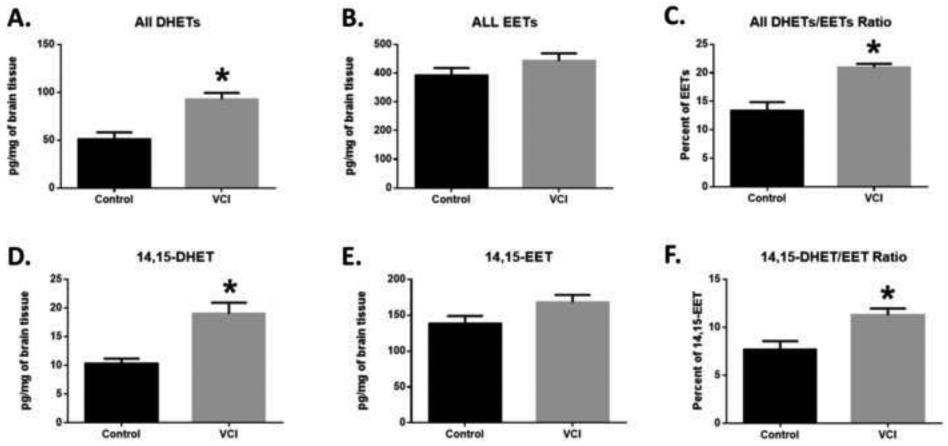


**Figure 3. Eicosanoid concentrations in control and VCI brain tissue**

Quantification of total DHETs (A), total EETs (B), total DHETs/total EETs Ratio (C), 14,15-DHET (D), 14,15-EET (E), and 14,15-DHET/14,15-EET ratio (F) (n= 5 separate brains per group). Data are graphed as mean +/−SEM. Significance was determined by an Mann-Whitney non-parametric test. * indicates $p<.05$.

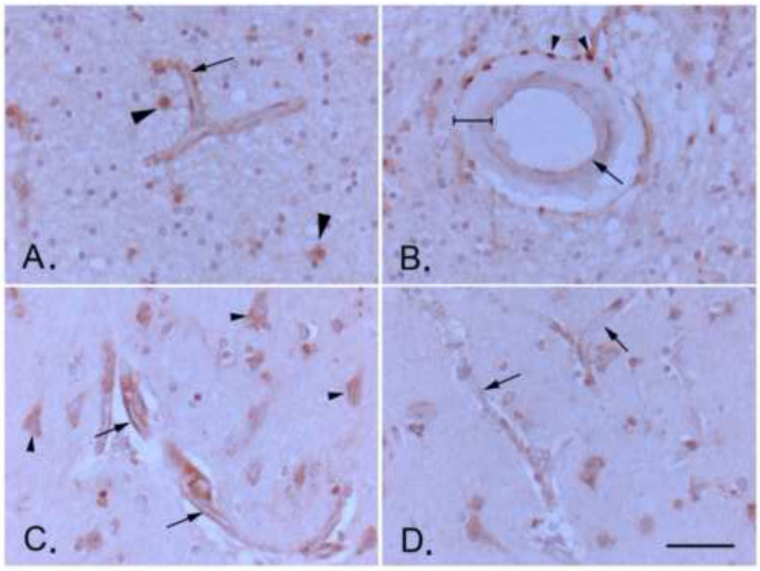


**Figure 4. Expression of soluble epoxide hydrolase (sEH) in the aged human brain**

A. Endothelial staining of a white matter microvessel, likely capillary (arrow; approximate diameter 10 μm; see scale bar in D.). Other immune-positive cells in the image include astrocytes (arrowheads). B. Immunohistochemical staining of a human brain surface pial arteriole (approximate diameter of 150 μm; see scale bar in D.) showing positive staining in perivascular adventitial cells (arrowheads, likely inflammatory cells), but only weak staining in endothelial cells (arrow; compare to microvascular staining in A., which is taken from the same brain section), and no staining in tunica media vascular smooth muscle (bracketed). C. and D. Microvascular endothelial staining shows is intensified near a cortical microinfarct (arrows in C.) compared to staining in control microvessels in the same brain section away from the microinfarct (arrows in D.). Arrowheads in C. point to neurons, staining of which does not intensify near lesion. Scale bar represents 50μm. All images are at the same magnification.

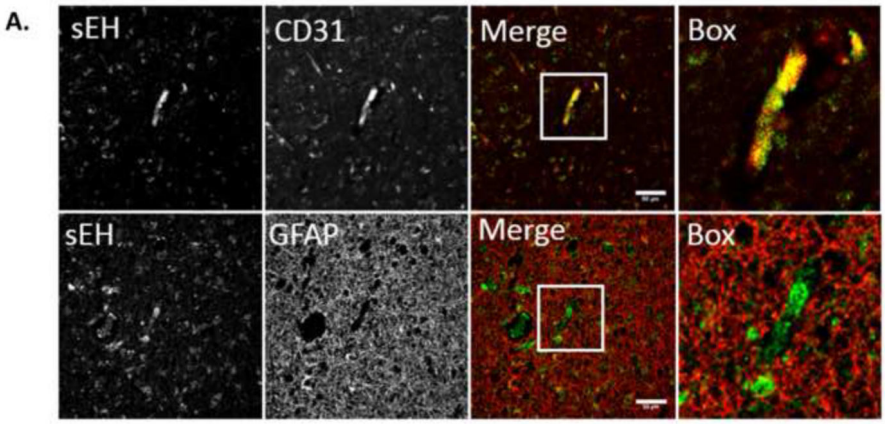


**Figure 5. Endothelial localization of soluble epoxide hydrolase (sEH) immunoreactivity (IR) in human brain microvessels**

A. Double-fluorescent immunohistochemistry of human brain tissue co-localizes sEH-IR (green) with the endothelial marker CD31 (platelet endothelial cell adhesion molecule, PECAM-1, red in upper panel) but not the astrocyte marker GFAP (glial fibrillary acidic protein, red in lower panel). Scale bar represents 50μm.

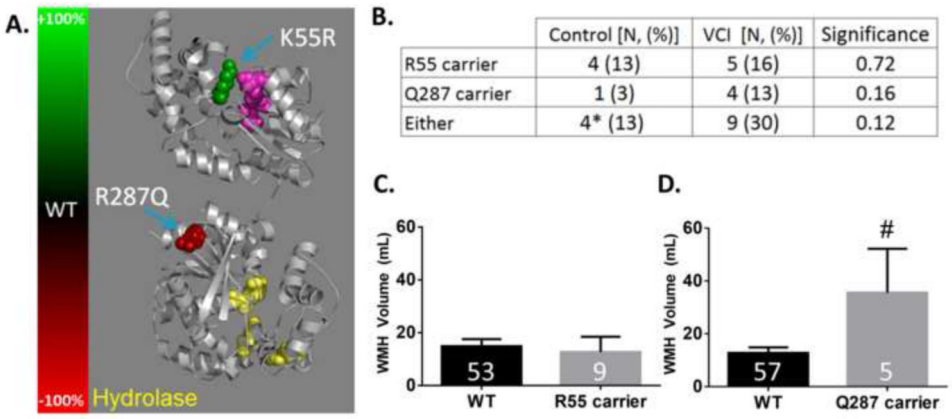


| | Control [N, (%)] | VCI [N, (%)] | Significance |
|---|---|---|---|
| R55 carrier | 4 (13) | 5 (16) | 0.72 |
| Q287 carrier | 1 (3) | 4 (13) | 0.16 |
| Either | 4* (13) | 9 (30) | 0.12 |

**Figure 6. EPHX2 functional missense polymorphisms in control and VCI subjects**

A. Crystal structure of sEH (PBD ID: 1S8O) [42] with change in hydrolase activity resulting from K55R and R287Q residues represented in color (green depicts increased activity and red depicts reduced activity). The hydrolase catalytic site is colored in yellow, and residues in the phosphatase catalytic site are colored in purple. B. Number of individuals carrying one or two sEH polymorphisms in control and VCI subjects. Number of individuals with a polymorphism is followed by the percentage within each group in parentheses. * Indicates that one control subject was a compound heterozygote, carrying both R55 and Q287. Significance was determined by a Chi-squared test, and p-values are provided in the significance column. n=31 for both control and VCI groups. C. Quantification of WMH volume by EPHX2 genotype at the amino acid 55 locus. WT indicates an individual with the most frequent allele, K55. D. Quantification of WMH volume by EPHX2 genotype at the amino acid 287 locus. WT indicates an individuals with the most frequent allele, R287. Numbers in the bar graph indicates the number of individuals in each group. Significance was determined by Student's t-test. # indicates $p<0.05$ compared to WT.

## Table 1

Demographic data of subjects used for mass spectrometry-based eicosanoid analysis.

| Group | N | Mean age (range) | % Male | Postmortem interval (range) |
|---|---|---|---|---|
| Controls | 5 | 95.8 (91-104) | 80% | 0.2 to 1.5 days |
| VCI | 5 | 94.6 (88-108) | 20% | 0.1 to 1 day |

## Table 2

Demographic data of subjects used for immunohistochemistry.

| Group | N | Mean age (range) | % Male | Postmortem interval (range) |
|---|---|---|---|---|
| Controls | 11 | 89.1 (79-96) | 45% | 0.2 to 1 day |
| VCI | 16 | 92.6 (87-106) | 44% | 0.2 to 8 days |

**Table 3**

Vascular injury scoring scale.

| Region | Arteriolosclerosis | Perivascular hemosiderin | Perivascular space dilatation | Myelin pallor | Cortical infarcts |
|---|---|---|---|---|---|
| Frontal | 0-3 | 0-3 | 0-3 | 0-3 | Number (up to 3) |
| Temporal | 0-3 | 0-3 | 0-3 | 0-3 | Number |
| Basal ganglia | 0-3 | | 0-3 | | Number |
| | | Neuron loss | | | |
| Hippocampus | | 0-3 | 0-3 | | Number |